

**Influence of ro-vibrational and isotope effects on the dynamics of the**  
 **$C(^3P) + OD(X^2\Pi) \rightarrow CO(X^1\Sigma^+) + D(^2S)$**   
**reaction**

Journal:	<i>Molecular Physics</i>
Manuscript ID:	TMPH-2010-0355.R1
Manuscript Type:	Full Paper
Date Submitted by the Author:	19-Oct-2010
Complete List of Authors:	Jorfi, Mohamed; University of Franche-Comte Honvault, Pascal; University of Franche-Comte, UFR ST Bussery-Honvault, Beatrice; Institut UTINAM, UMR CNRS 6213, Faculté des Sciences et Techniques Banares, Luis; Universidad Complutense de Madrid Bulut, Niyazi; Firat University
Keywords:	reaction dynamics, gas phase reactions, quantum dynamics, reactive collisions
Note: The following files were submitted by the author for peer review, but cannot be converted to PDF. You must view these files (e.g. movies) online.	
source files.zip	

1  
2  
3  
4  
5  
6  
7  
8  
9  
10  
11  
12  
13  
14  
15  
16  
17  
18  
19  
20  
21  
22  
23  
24  
25  
26  
27  
28  
29  
30  
31  
32  
33  
34  
35  
36  
37  
38  
39  
40  
41  
42  
43  
44  
45  
46  
47  
48  
49  
50  
51  
52  
53  
54  
55  
56  
57  
58  
59  
60

For Peer Review Only

1  
2  
3 **Influence of ro-vibrational and isotope effects on the dynamics of**  
4  
5 **the  $C(^3P)+OD(X^2\Pi) \rightarrow CO(X^1\Sigma^+) + D(^2S)$  reaction**  
6  
7

8 Mohamed Jorfi, Pascal Honvault\*, and Béatrice Bussery-Honvault  
9  
10 *Institut UTINAM, UMR CNRS 6213, University of Franche-Comté,*  
11  
12 *UFR Science et Techniques, 25030 Besancon cedex, France*  
13

14  
15 Luis Bañares  
16  
17 *Departamento de Química Física, Facultad de Química,*  
18  
19 *Universidad Complutense, 28040 Madrid, Spain*  
20

21  
22 Niyazi Bulut†  
23  
24 *Firat University, Department of Physics, 23169 Elaziğ, Turkey*  
25

26 (Dated: October 19, 2010)

27  
28 **Abstract**

29  
30 The  $C(^3P)+OD(X^2\Pi)$  reaction has been studied by means of quantum mechanical real wave  
31 packet (RWP) and quasiclassical trajectory (QCT) methodologies on the ground potential energy  
32 surface of Zanchet *et al.* [J. Phys. Chem. A **110**, 12017 (2006)]. Initial state selected total  
33 reaction probabilities at  $J = 0$  total angular momentum have been calculated for a wide range  
34 of collision energies. Product state-resolved integral cross sections at selected collision energies  
35 and excitation functions have been determined from the RWP calculations using the  $J$ -shifting  
36 approximation and from QCT calculations. State-specific and thermal rate coefficients have been  
37 calculated using both methodologies up to 500 K. The effect of reagent rotational excitation on  
38 the dynamics for the  $C(^3P)+OH(X^2\Pi)$  and  $C(^3P)+OD(X^2\Pi)$  reactions has been investigated and  
39 interesting discrepancies between the QCT and RWP results have been found. The RWP results  
40 are found to be in an overall good agreement with the corresponding QCT results, although the  
41 QCT integral cross-section and rate coefficients are slightly smaller than those obtained from the  
42 RWP calculations.  
43  
44  
45  
46  
47  
48  
49  
50  
51  
52  
53  
54  
55  
56  
57

58 \_\_\_\_\_  
59 \* e-mail: pascal.honvault@univ-fcomte.fr

60 † e-mail: nbulut@firat.edu.tr

## I. INTRODUCTION

The reaction of open-shell C atoms with OH radicals is of fundamental importance in the production of carbon monoxide in various chemical environments and, particularly, in astrophysics and interstellar clouds[1–4]. Quantum mechanical (QM) reactive scattering studies of reactions involving open-shell species require the availability of a high level global three dimensional *ab initio* potential energy surface (PES). In addition, this type of reaction usually involves PESs characterized by the presence of a deep potential well and heavy atoms, which makes QM calculations very challenging since many channels have to be considered to get well converged results [3].

The first global *ab initio* PES for the  $C(^3P)+OH(X^2\Pi)$  reaction was built by Zanchet *et al.* [1]. This PES is based on about 2000 *ab initio* points computed at the multireference (MR) internally contracted single and double configuration interaction level plus Davidson correction using Dunning aug-cc-pVQZ basis sets [1]. The MR space was taken to be a complete active space (CAS). The *ab initio* points were fit using the reproducing kernel Hilbert space (RKHS) methodology [5].

Theoretical studies of reactive collision between open-shell and halogen atoms with  $H_2$  molecule and hydroxyl radical, OH, has been extensively studied [6–9]. In theoretical studies on interaction between open-shell atoms with OH molecules, several electronic states participate in the dynamics. These several electronic states many times responsible for non-Born-Oppenheimer effects [9]. Approach of the OH molecule to the C atom split the degeneracy of the  $^3P$  state. As shown and described in Table 1 and Figure 1. in [1] the entrance channel of the  $C(^3P)+OH(X^2\Pi)$  reaction gives to six doublet states and six quarter states which are correlated in  $C_\infty v$  to  $^2,4\Sigma^+$ ,  $^2,4\Sigma^-$ , and  $^2,4\Delta$  states. Each  $\Pi$  and  $\Delta$  state will split into one  $A'$  and  $A''$  state in the  $C_s$  symmetry group while the  $\Sigma^+$  state leads to one  $A'$  and the  $\Sigma^-$  state to one  $A''$  state. So, in  $C_s$ , the title reaction will lead to three  $^2A'$  and three  $^2A''$  states and most of these states present considerable higher in energy and energetically inaccessible.  $C(^3P)+OH(X^2\Pi)$  reactant correlate adiabatically with the ground state of the products  $CO(X^1\Sigma_g^+)+H(^2S)$  due to the nondegenerate states.

The  $C(^3P)+OH(X^2\Pi) \rightarrow CO(X^1\Sigma^+)+H(^2S)$  reaction is highly exothermic ( $\approx 6.4$  eV) and barrierless relative to the entrance channel, while three minima and five potential barriers are located on the surface. The three minima correspond to the formation of HCO and

1  
2  
3 COH complexes and to the CO+H products, with the COH complex being a metastable  
4 minimum relative to the product channel. The five saddle points correspond to potential  
5 barriers for both the dissociation/formation of HCO and COH into/from CO+H, to barriers  
6 for the isomerization of HCO into COH and to barriers for the inversion of HCO and COH  
7 through their respective linear configurations.  
8  
9

10  
11  
12 The first theoretical cross sections and rate coefficients on this PES were calculated  
13 by Zanchet *et al.* employing the quasiclassical trajectory (QCT) method [2]. Total and  
14 state-specific integral cross-sections were calculated as a function of collision energy. The  
15 calculated thermal rate coefficients were found to be practically temperature independent at  
16 high enough temperatures and almost invariant on the ro-vibrational state of the OH reagent.  
17 Employing this same PES, Zanchet *et al.* [3] performed QCT calculations of differential cross  
18 sections (DCS) and product energy distributions in a wide range of collision energies, and the  
19 influence of the reagent diatom ro-vibrational excitation on these quantities was explored.  
20 It was found that ro-vibrational excitation of OH has no effect on the product vibrational,  
21 rotational and translational distributions, but DCSs show a weak dependency on the initial  
22 rotational state of the reagent molecule. An analysis of the results was performed in terms  
23 of the lifetimes of the intermediate complexes and on the kinematic constraints associated  
24 with the mass combination.  
25  
26

27  
28  
29  
30  
31  
32  
33  
34  
35  
36  
37  
38  
39  
40  
41  
42  
43  
44  
45  
46  
47  
48  
49  
50  
51  
52  
53  
54  
55  
56  
57  
58  
59  
60

Lin *et al.* performed the first exact wave packet calculations on the same PES for total  
angular momentum  $J = 0$  using a flux analysis method [4]. These calculations were carried  
out using reactant Jacobi coordinates. The total reaction probability as a function of collision  
energy was calculated without resolving the final states of the products. It was found that the  
dynamics of the title reaction is dominated by the capture of the reactants and calculations  
at  $J \geq 0$  were carried out using a capture model. The reported integral cross sections and  
rate coefficients were found in good agreement with the earlier QCT results except at low  
collision energies and low temperatures, respectively.

In a recent work, Bulut *et al.* [25] carried out real wave packet (RWP) and QCT calcula-  
tions for the  $C(^3P)+OH(X^2\Pi)$  reaction on the PES of Zanchet *et al.*[1] at the state-to-state  
level. The wave packet calculations were performed using product Jacobi coordinates at  
zero total angular momentum,  $J = 0$ , in order to obtain state-to-state reaction probabili-  
ties. State-to-state integral cross sections were computed using a capture model[4, 11]. The  
corresponding state-selected rate coefficients were calculated by Boltzmann averaging of the

1  
2  
3 integral cross sections. The RWP results were thoroughly compared with QCT calculations  
4 on the same PES.  
5

6  
7 In the present work, the real wave packet (RWP) and QCT methods have been applied to  
8 study the dynamics of the  $C(^3P)+OD(X^2\Pi)$  isotopic variant of the reaction on the same PES  
9 at the state-to-state level. Integral cross sections and rate coefficients have been evaluated  
10 using the same methodologies as in Ref. [25]. Detailed comparisons between the two methods  
11 and for the two isotopic variants have been carried out.  
12  
13  
14

15  
16 The organization of the paper is as follows: in section II we will briefly review the RWP  
17 and QCT theoretical methods employed in this work, section III will present the results and  
18 discussion and finally section IV will close with the conclusions.  
19  
20  
21

## 22 23 **II. THEORY**

### 24 25 **A. Real wave packet method**

26  
27 The real wave packet (RWP) calculations have been performed using the method devel-  
28 oped by Gray and Balint-Kurti[10]. As the RWP method has been well documented in the  
29 literature[10, 12, 13] and in our previous work [25]for the C+OH reaction, we summarize  
30 here only the most relevant details for the present study.  
31  
32

33  
34 For the present calculations, the initial wave packet is located in the asymptotic reactant  
35 channel, where there is no influence of the interaction potential, and the propagation grid  
36 scheme is defined using the product Jacobi coordinates. The calculations have been carried  
37 out over a broad range of collision energies. The properties of the initial wave packet and  
38 the parameters used for the calculations are given in Table I.  
39  
40  
41  
42

43  
44 RWP integral cross sections and rate coefficients have been evaluated using the same  
45 methodologies as in Ref. [25]. RWP calculations have been performed for total angular  
46 momentum  $J = 0$ . A variant of the standard J-shifting method has been applied to estimate  
47 reaction probabilities for  $J > 0$  and integral cross sections as a function of collision energy  
48 and rate coefficients have been calculated from the state-to-state reaction probabilities.  
49  
50  
51  
52  
53  
54  
55  
56  
57  
58  
59  
60

## B. Quasiclassical trajectory calculations

The QCT code developed by Halvick and Rayez [22] has been used for the calculation of reaction probabilities, cross sections and rate coefficients [1–3, 25] and we summarize here only the most relevant details for the present study.

The QCT calculations employ a standard Monte Carlo sampling of the initial conditions and the step adaptive Adams method for the integration of the set of Hamilton equations. Conservation of both total energy and angular momentum has been checked for each trajectory. At each integration step, a relative precision of  $10^{-9}$  for distances and momenta have been required, which yields a conservation of total energy and total angular momentum with an average error of  $10^{-5}$  eV and  $10^{-6} \hbar$ , respectively. The high number of trajectories ( $N_t=100000$ ) together with the high efficiency of the trajectories (number of reactive trajectories/ $N_t = 3/5$ ) gives a statistical Monte Carlo error of 0.15%. The carbon atom is initially separated from the center-of-mass of OD by 12 Å for the highest collision energies and 21 Å for the lowest ones. The trajectories are stopped when the recoil distance is larger than 10 Å and the recoil speed is quasi constant. These values have been chosen in order to have negligible long range interactions. Preliminary batches of 500 trajectories were performed for each collision energy with a large maximum impact parameter. Then batches of 100000 trajectories have been run with the appropriate value of the maximum impact parameter which varies from 10.5 to 3.5 Å as energy increases. To check the validity of the number of trajectories chosen in our study, calculations of cross sections for  $C+OD(v=0, j=0)$  at a few translational energies have been carried out by running 200000 trajectories in order to reduce statistical errors. The results obtained with 100000 trajectories are coincident and quasi-identical to those obtained with 200000 trajectories.

The quantum numbers  $v'$  and  $j'$  of the diatomic CO product have been assigned using the usual histogrammatic binning method, which consists in rounding the vibrational and rotational classical actions to the nearest integer. This procedure is one of the major shortcomings of the QCT method. However, significant errors are only observed when the number of open rovibrational channels of the products is small. The title reaction is not very much concerned by this drawback as long as we are interested in the D+CO reactive channel and not in the O+CD channel.

The calculations of state-to-state integral cross sections and rate coefficients have been

1  
2  
3 carried out as outlined in Refs. [2, 3].  
4  
5  
6

### 7 III. RESULTS AND DISCUSSION

#### 8 A. Total and state-to-state reaction probabilities at $J = 0$

9  
10  
11  
12  
13 Total reaction probabilities as a function of collision energy calculated using the RWP and  
14 QCT methodologies for the C+OD( $v = 0, j = 0, 1, 5$ ) reactions at total angular momentum  
15  $J = 0$  are depicted in Figure 1. As for the C+OH reaction [25], the reaction probabilities  
16 show no threshold, as expected for a barrierless reaction, reaching values around 1 just above  
17 the lowest collision energies calculated (steplike behavior). This reveals that the reaction  
18 is dominated by the capture of the reagents due to the large exothermicity and barrierless  
19 character of the PES. Some oscillatory behavior is observed in the RWP reaction probabilities  
20 over the whole range of collision energies, although the amplitude of the structures decreases  
21 with increasing collision energy. To check the effect of a fine grid bases on these oscillatory  
22 some tests calculations have been performed with large ro-vibrational basis and with large  
23 dimension of radial grid and Legendre basis. After many test, we converged the reaction  
24 probabilities at zero total angular momentum,  $J = 0$ , with the parameters and basis of the  
25 Table 1. The origin of these structures cannot be attributed to real resonances but to the  
26 incomplete damping of the outgoing wave packet [4]. It is found that both RWP and QCT  
27 probabilities slightly decrease with increasing collision energy for all  $j$  values considered and  
28 the QCT probabilities reproduce the overall shape of the RWP results, but the former are  
29 somewhat smaller than the latter. This behavior is more marked for this isotopic variant  
30 than for the C+OH reaction and the influence of the initial rotational excitation of the OD  
31 reagent is very minor and without a clear tendency, as in the C+OH case [25].  
32  
33  
34  
35  
36  
37  
38  
39  
40  
41  
42  
43  
44  
45  
46

47 Figure 2 shows RWP and QCT reaction probability product vibration distributions  
48 calculated at  $J = 0$  and selected collision energies (0.01, 0.05, 0.1, 0.5 eV) for the  
49 C+OD( $v = 0, j = 0$ ) reaction. As can be seen, the state-resolved reaction probabilities  
50 show a similar structure and a substantial product vibrational excitation is observed with a  
51 clear population inversion. As collision energy increases, the RWP vibrational distributions  
52 are hotter, becoming wider and peaking at higher  $v'$  values. The QCT vibrational distribu-  
53 tions reproduce the overall shape of the RWP distributions at all collision energies, except  
54  
55  
56  
57  
58  
59  
60



1  
2  
3 integral cross-sections for both C+OH and C+OD reactions are slightly smaller than the  
4 RWP ones in the whole range of collision energies. It is interesting to notice that the QCT  
5 and RWP cross-sections for the C+OD reaction are smaller than those obtained for the  
6 C+OH reaction in the whole collision energy range, which indicates an isotope effect (de-  
7 fined as  $\Gamma = \sigma_{\text{CO+H}}/\sigma_{\text{CO+D}}$ ) larger than one. This result is in contrast with that found  
8 for the insertion barrierless  $\text{S}(^1D)+\text{H}_2/\text{D}_2$  reaction, where no significant isotope effect was  
9 found [27]. No isotope effect would be expected for a typical statistical insertion reaction.  
10 The fact that a positive isotope effect is found for the C+OH/OD reactions indicates that  
11 this system deviates from a statistical behavior.  
12  
13  
14  
15  
16  
17  
18

19 The computed vibrationally state-resolved integral cross-sections at selected collision en-  
20 ergies for the C+OD( $v=0, j=0$ ) reaction are plotted in Figure 6. The RWP vibrational  
21 distributions peak at high values of  $v'$  showing population inversion. It is clear that the  
22 RWP plots of ICSs at constant collision energies as a function of product vibrational quan-  
23 tum number show a bimodality at low collision energies of 0.01 eV, 0.05 eV and 0.1 eV while  
24 the QCT ICSs display a monomodal behavior at all collision energies. The agreement found  
25 between the RWP and QCT vibrational distributions is rather good at 0.01 eV collision en-  
26 ergy. However, at the higher collision energies (0.05, 0.1 and 0.5 eV), the QCT vibrational  
27 distribution peaking at lower rotational quantum numbers. As collision energy increases,  
28 more and more low vibrational states are populated in the QCT distributions and the peak  
29 of the distributions is shifted toward lower  $v'$  values. This behavior has been observed in  
30 our previously for the C+OH reaction [25].  
31  
32  
33  
34  
35  
36  
37  
38  
39  
40  
41  
42

### 43 C. Rate coefficients

44  
45 Initial rotational state-selected rate coefficients in the temperature range 0-500 K have  
46 been calculated from the corresponding RWP and QCT excitation functions using Eq.(6)  
47 and considering Eq. (7) in Ref. [25] for the electronic partition function and are depicted in  
48 Figure 7. As can be seen, both RWP and QCT state-selected rate coefficients first increase  
49 at the lowest temperatures up to 20 K and 7 K respectively. Then they decrease slightly with  
50 increasing temperature reaching an almost constant value at 150 K. Similar findings have  
51 been reported for the C+OH isotope variant of the reaction [25]. The QCT rate coefficients  
52 are slightly lower than the RWP ones in the studied range of temperatures. The RWP and  
53  
54  
55  
56  
57  
58  
59  
60

1  
2  
3 QCT state-selected rate coefficients for the title reaction are only slightly dependent on the  
4 initial rotational quantum number of the reagent molecule. The agreement found between  
5 RWP and QCT rate coefficients is good at temperatures above about 100 K.  
6  
7

8  
9 The corresponding RWP rate constants obtained by statistically averaging over the ro-  
10 tational states  $j = 0 - 5$  have been calculated using Eq.(8) in Ref. [25] and are displayed  
11 in Figure 8 for both the C+OH and C+OD reactions. The corresponding QCT rate coef-  
12 ficients for the C+OD reaction are also depicted in the figure. As found for the integral  
13 cross sections, a positive isotope effect is found for the C+OH/C+OD reaction, the C+OH  
14 rate coefficients being somewhat larger than those for the C+OD reaction. In any case,  
15 both RWP and QCT  $k(T)$  values are almost independent on temperature for  $T > 200$  K.  
16 In general, the QCT rate coefficients are smaller than those obtained by the RWP method.  
17 The agreement is increasingly better at temperature increases.  
18  
19  
20  
21  
22  
23  
24  
25  
26

#### 27 IV. CONCLUSIONS

28  
29 Initial state selected total reaction probabilities, product state-resolved integral cross  
30 sections at selected collision energies (0.01, 0.05, 0.1, 0.5 eV), integral cross-sections as a  
31 function of collision energy and rate coefficients for the reaction  $C+OD \rightarrow CO+D$  have been  
32 computed using a time dependent real wave packet method and the quasi-classical trajectory  
33 approximation on the ground PES of Zanchet *et al.* [J. Phys. Chem. A **110**, 12017(2006)].  
34 The integral cross-section values for C+OD obtained from RWP and QCT calculations are  
35 nearly the same at high collision energies. It has also been found that the dynamics is  
36 not very sensitive to the choice of initial  $j$  values considered, except at very low energy or  
37 temperature.  
38  
39  
40  
41  
42  
43  
44  
45

46 Some interesting discrepancies between the QCT methodology and RWP calculations  
47 have been found. Of course, the QCT method is ambiguous in the treatment of the ZPE  
48 in the product channel. In addition, this classical method ignores possible tunneling effects,  
49 which are fully accounted for in the QM calculations. For the RWP side, errors can be  
50 appear at very low collision energy because of the incomplete damping of the slowly moving  
51 components of the wave packet. Finally, the RWP cross sections and rate constants have  
52 been calculated using the  $J$ -shifting approximation. A first necessary improvement is the  
53 removal of such an approximation. Work in these directions is underway in our groups.  
54  
55  
56  
57  
58  
59  
60

**ACKNOWLEDGMENTS**

This work has been supported by the Scientific and Technological Research Council of TURKEY (TUBITAK) and Firat University Scientific Research Projects Unit (FUBAP) under Project Nos. TBAG-109T447 and FUBAP-1775. Partial financial support from the Spanish Ministry of Science and Innovation (CTQ2008-02578/BQU) is gratefully acknowledged. The QCT calculations were performed using HPC resources from GENCI [CCRT/CINES/IDRIS] (Grant 2010 [i2010082031]). Computations have also been done on the Mesocentre de calcul de Franche-Comté machine.

- 
- 1  
2  
3  
4  
5  
6  
7 [1] A. Zanchet, B. Bussery-Honvault, and P.Honvault, *J. Chem. Phys. A.*, **110**,12017(2006).  
8  
9 [2] A. Zanchet, P. Halvick, J. C. Rayez, B. Bussery-Honvault, and P.Honvault, *J. Chem.*  
10 *Phys.*,**126**,184308(2007).  
11  
12 [3] A. Zanchet, P. Halvick, B. Bussery-Honvault, and P.Honvault, *J. Chem.*  
13 *Phys.*,**128**,204301(2008).  
14  
15 [4] S. Y. Lin H. Guo, P. Honvault, *Chem.Phys. Lett.*, **453** , 140 (2008).  
16  
17 [5] T.-S. Ho and H. J. Rabitz, *Chem. Phys.* **104**, 2584 (1996).  
18  
19 [6] B. Bussery-Honvault, P. Honvault and J.-M. Launay, *J.Chem.Phys.*, **115**,10701 (2001).  
20  
21 [7] P. Honvault and J.-M. Launay, *J.Chem.Phys.*, **114**,1057 (2001).  
22  
23 [8] Z. Sun, D.H. Zhang, M.H. Alexander, *J.Chem.Phys.*, **132**,034308 (2010).  
24  
25 [9] M.H. Alexander, G. Capecchi, H.-J. Werner, *Faraday Diss.*, **127**,59(2004).  
26  
27 [10] S. K. Gray and G. G. Balint-Kurti, *J. Chem. Phys.* **108**, 950 (1998).  
28  
29 [11] S. K. Gray,E. M. Goldfield, G. C. Schatz, and G. G. Balint-Kurti, *Phys. Chem. Chem. Phys*,  
30 **1**, 1141, (1999).  
31  
32 [12] G. G. Balint-Kurti, A. I. Gonzalez, E. M. Goldfield and S. K. Gray, *Faraday Discuss.* **110**,  
33 169 (1998).  
34  
35 [13] M. Hankel, G. G. Balint-Kurti and S. K. Gray, *Int. J. Quantum Chem.* **92**, 205 (2003).  
36  
37 [14] Y. Huang, D.J.Kouri, and D.K. Hoffman, *J.Chem.Phys.* **101**, 10493 (1994).  
38  
39 [15] Y. Huang, S.S.Iyengar, D.J.Kouri, and D.K. Hoffman, *J.Chem.Phys.* **105**, 927 (1996).  
40  
41 [16] V. A. Mandelshtam and H. S. Taylor, *J. Chem. Phys.* **102**, 7390 (1995).  
42  
43 [17] V. A. Mandelshtam and H. S. Taylor, *J. Chem. Phys.* **103**, 2903 (1995).  
44  
45 [18] G. J. Kroes and D. Neuhauser, *J. Chem. Phys.* **105**, 8890 (1998).  
46  
47 [19] R. Chen and H.Guo, *J. Chem. Phys.* **105**, 3569 (1996).  
48  
49 [20] S.C. Althorpe, *J. Chem. Phys.* **114**, 1601 (2001).  
50  
51 [21] M. Hankel, G.G.Balint-Kurti, S.K.Gray, *J. Chem. Phys.*, **113**, 9658 (2000).  
52  
53 [22] Ph. Halvick and J.-C. Rayez, *Chem. Phys.*, **131**, 375 (1989).  
54  
55 [23] M. Jorfi, P. Honvault, P. Halvick, S. Y. Lin, H. Guo, *Chem. Phys. Lett.*, **462**, 53 (2008).  
56  
57 [24] M. Jorfi, P. Honvault, P. Halvick, *Chem. Phys. Lett.*, **471**, 65 (2009).  
58  
59 [25] N. Bulut, A. Zanchet, P. Honvault, B. Bussery-Honvault and L. Bañares, *J. Chem. Phys.*,  
60

1  
2  
3  
4 **130**, 194303 (2009).

5 [26] N. Bulut, J. F. Castillo, F. J. Aoiz, and L. Bañares, Phys. Chem. Chem. Phys. , **10**, 821-827  
6  
7 (2008).

8  
9 [27] L. Bañares, J. F. Castillo, P. Honvault and J.-M. Launay, Phys. Chem. Chem. Phys., **7**, 627  
10  
11 (2005).  
12  
13  
14  
15  
16  
17  
18  
19  
20  
21  
22  
23  
24  
25  
26  
27  
28  
29  
30  
31  
32  
33  
34  
35  
36  
37  
38  
39  
40  
41  
42  
43  
44  
45  
46  
47  
48  
49  
50  
51  
52  
53  
54  
55  
56  
57  
58  
59  
60

For Peer Review Only

TABLE I: Parameters used in the RWP calculations (all parameters are given in atomic units).

Reactant scattering coordinate range:	$R_{min} = 0.1; R_{max} = 18.0$
Number of grid points in R:	255
Diatomic coordinate range:	$r_{min} = 0.7; r_{max} = 18.0$
Number of grid points in r :	479
Number of angular basis functions :	100
Center of initial wave packet :	$R_0 = 14.5$
Gaussian width factor :	$\alpha = 20.5$
Initial translational kinetic energy/eV :	$k_0 = 0.4$
Analysis point:	=10.0
Number of Chebyshev iterations:	70000

## FIGURES CAPTIONS

**Figure 1** Total reaction probabilities at  $J = 0$  as a function of collision energy calculated using the RWP and QCT methods for various initial rotational states of the OD( $v = 0$ ) radical for the title reaction.

**Figure 2** Final  $v'$  state-resolved reaction probabilities at  $J = 0$  for the C+OD( $v = 0, j = 0$ )  $\rightarrow$ CO( $v'$ )+D reaction at selected collision energies (0.01, 0.05, 0.1, 0.5 eV) obtained with the RWP (black squares) and QCT (open circles) methodologies.

**Figure 3** Final  $j'$  state-resolved reaction probabilities at  $J = 0$  for the C+OD( $v = 0, j = 0 - 5$ ) $\rightarrow$ CO( $v' = 14, j'$ )+D reactions at selected collision energies (0.01, 0.05, 0.1, 0.5 eV) obtained with the RWP method (black circles) and QCT method (red squares).

**Figure 4** Integral cross-sections as a function of collision energy for the C+OD( $v = 0, j = 0 - 5$ ) reactions calculated by the RWP and QCT methods.

**Figure 5** Integral cross-sections as a function of collision energy for the C+OD( $v = 0, j = 0$ ) and C+OH( $v = 0, j = 0$ ) reactions calculated by the RWP and QCT methods.

**Figure 6** Final  $v'$  state-resolved integral cross sections for the C+OD( $v = 0, j = 0 - 5$ )  $\rightarrow$ CO( $v'$ )+D reactions at selected collision energies (0.01, 0.05, 0.1, 0.5 eV) calculated with the RWP method (black squares) and QCT method (open squares).

**Figure 7** Rotationally state-specific rate coefficients as a function of temperature for the C+OD( $v = 0, j = 0 - 5$ ) reaction calculated with the RWP method (top panel) and the QCT method (bottom panel).

**Figure 8** Thermal rate constant as a function of temperature for the C+OD(OH) reaction calculated with the RWP method (red and black) and the QCT method (blue).

1  
2  
3  
4  
5  
6  
7  
8  
9  
10  
11  
12  
13  
14  
15  
16  
17  
18  
19  
20  
21  
22  
23  
24  
25  
26  
27  
28  
29  
30  
31  
32  
33  
34  
35  
36  
37  
38  
39  
40  
41  
42  
43  
44  
45  
46  
47  
48  
49  
50  
51  
52  
53  
54  
55  
56  
57  
58  
59  
60

FIG. 1: Jorfi et al.; Mol. Phys.

FIG. 2: Jorfi et al.; Mol. Phys.

FIG. 3: Jorfi et al.; Mol. Phys.

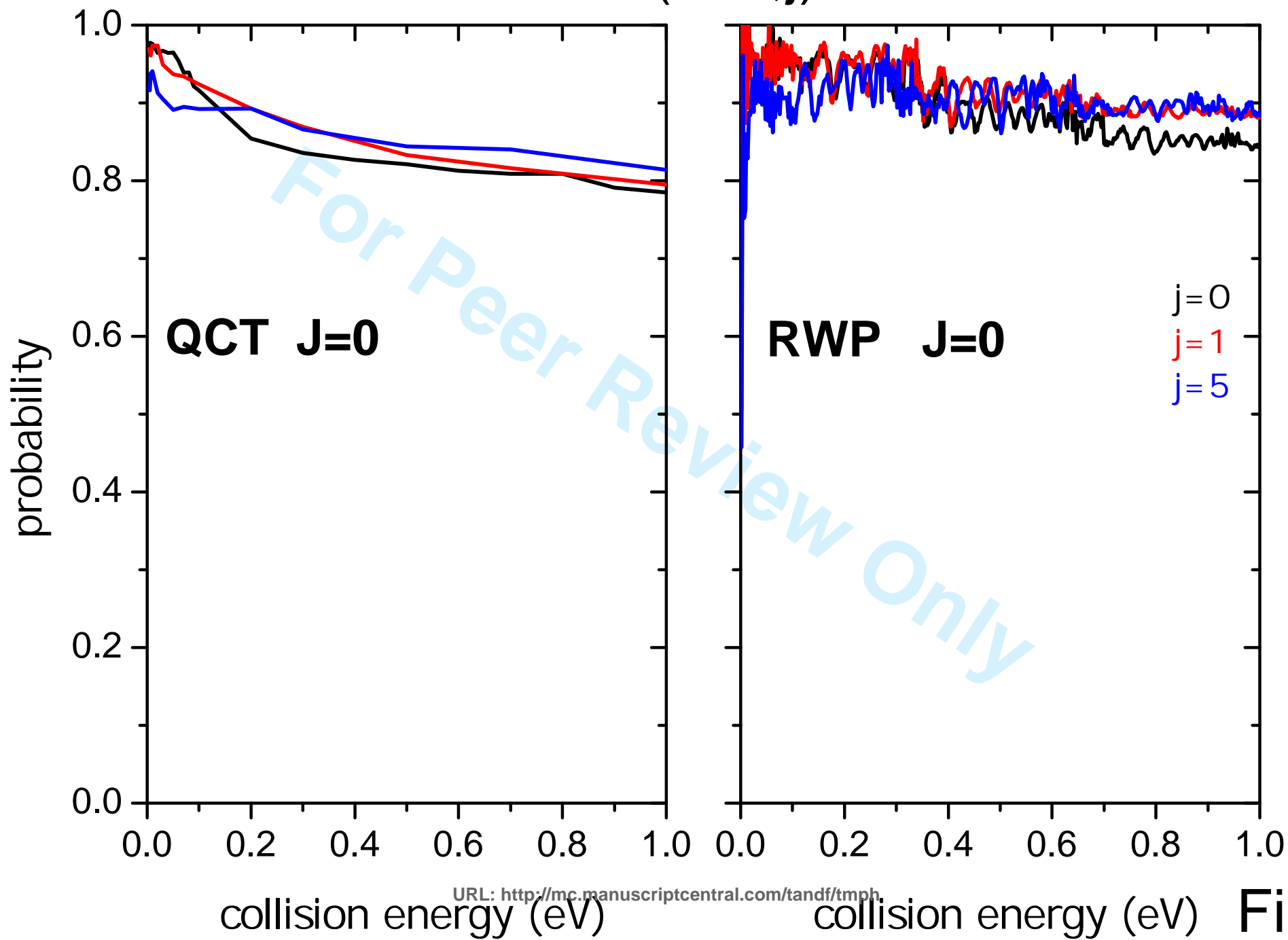
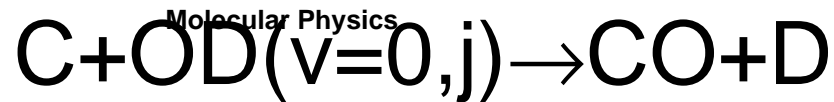
FIG. 4: Jorfi et al.; Mol. Phys.

FIG. 5: Jorfi et al.; Mol. Phys.

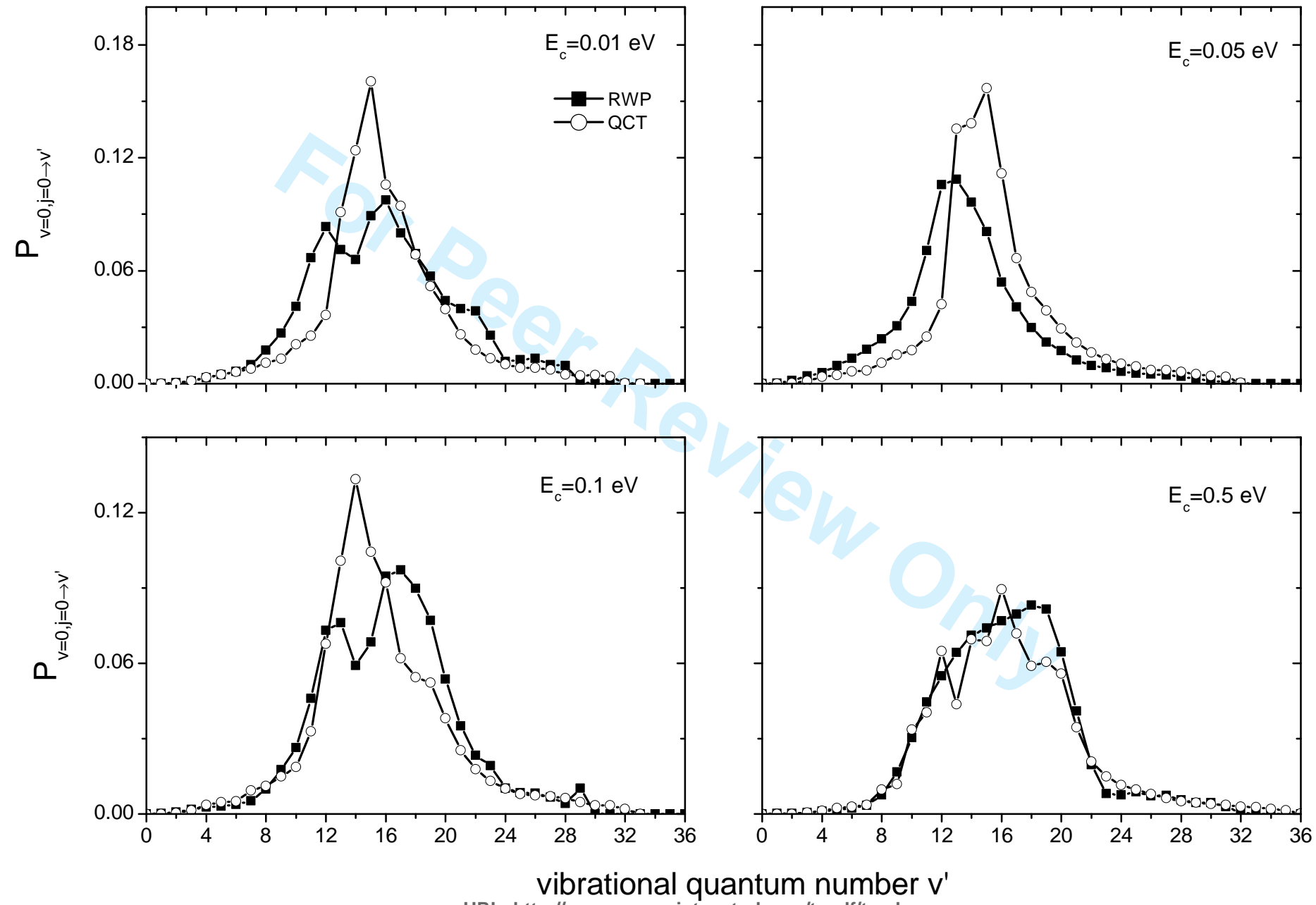
FIG. 6: Jorfi et al.; Mol. Phys.

FIG. 7: Jorfi et al.; Mol. Phys.

FIG. 8: Jorfi et al.; Mol. Phys.



1  
2  
3  
4  
5  
6  
7  
8  
9  
10  
11  
12  
13  
14  
15  
16  
17  
18  
19  
20  
21  
22  
23  
24  
25  
26  
27  
28  
29  
30  
31  
32  
33  
34  
35  
36  
37  
38  
39  
40  
41  
42  
43  
44  
45



URL: <http://mc.manuscriptcentral.com/tandf/tmph>

Fig.2

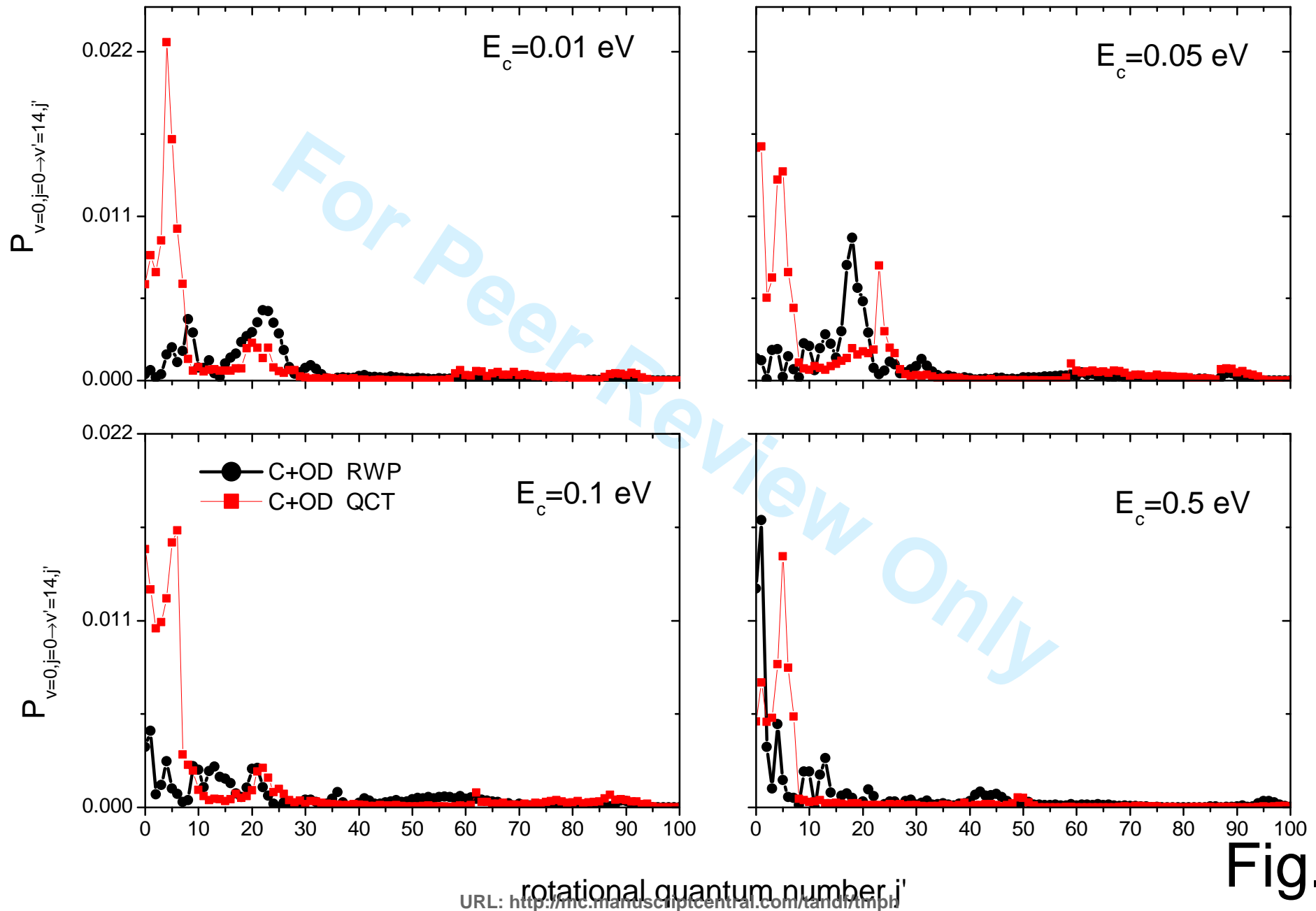
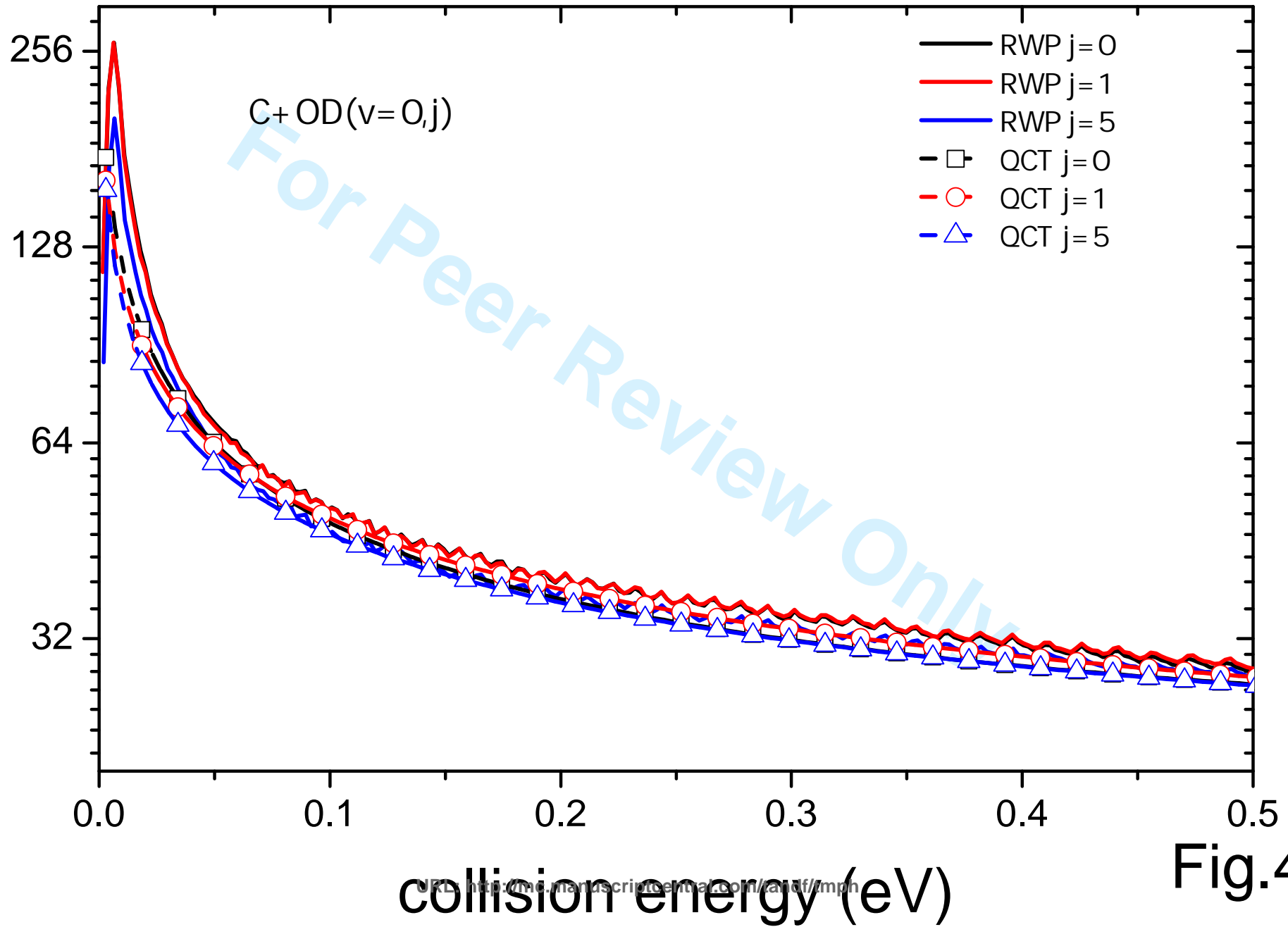
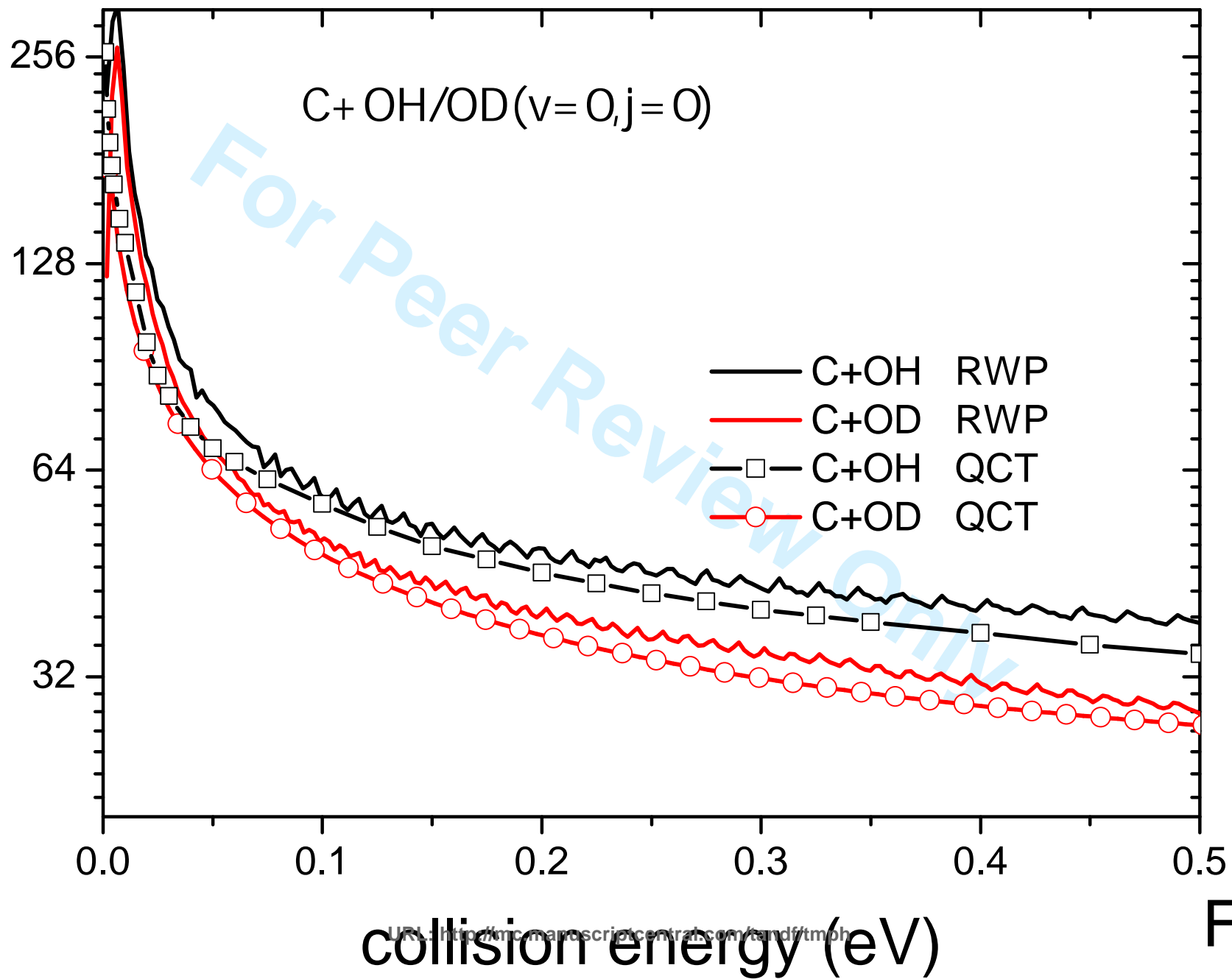
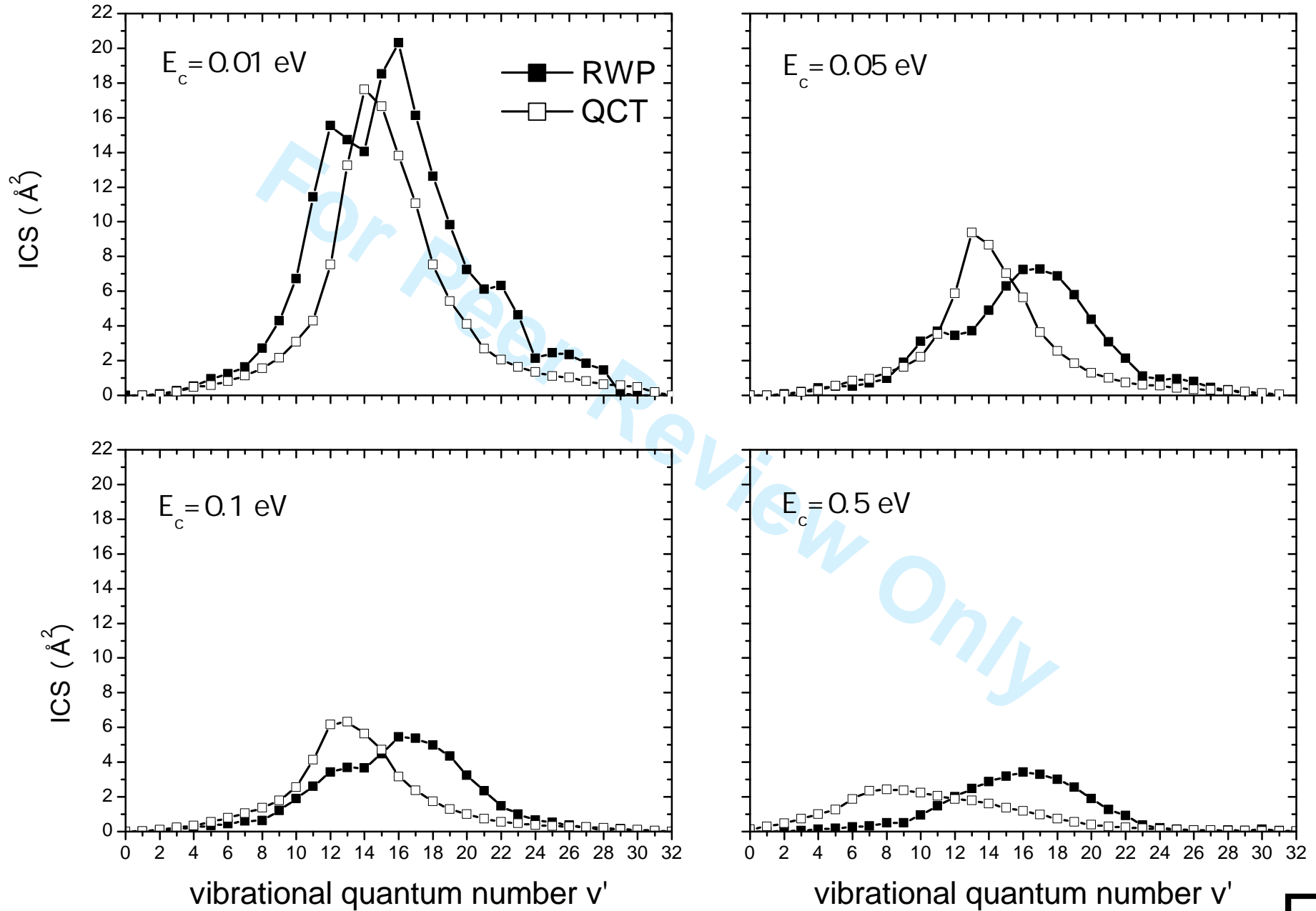
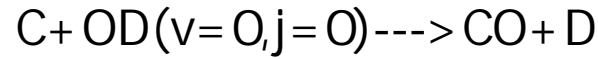


Fig.3







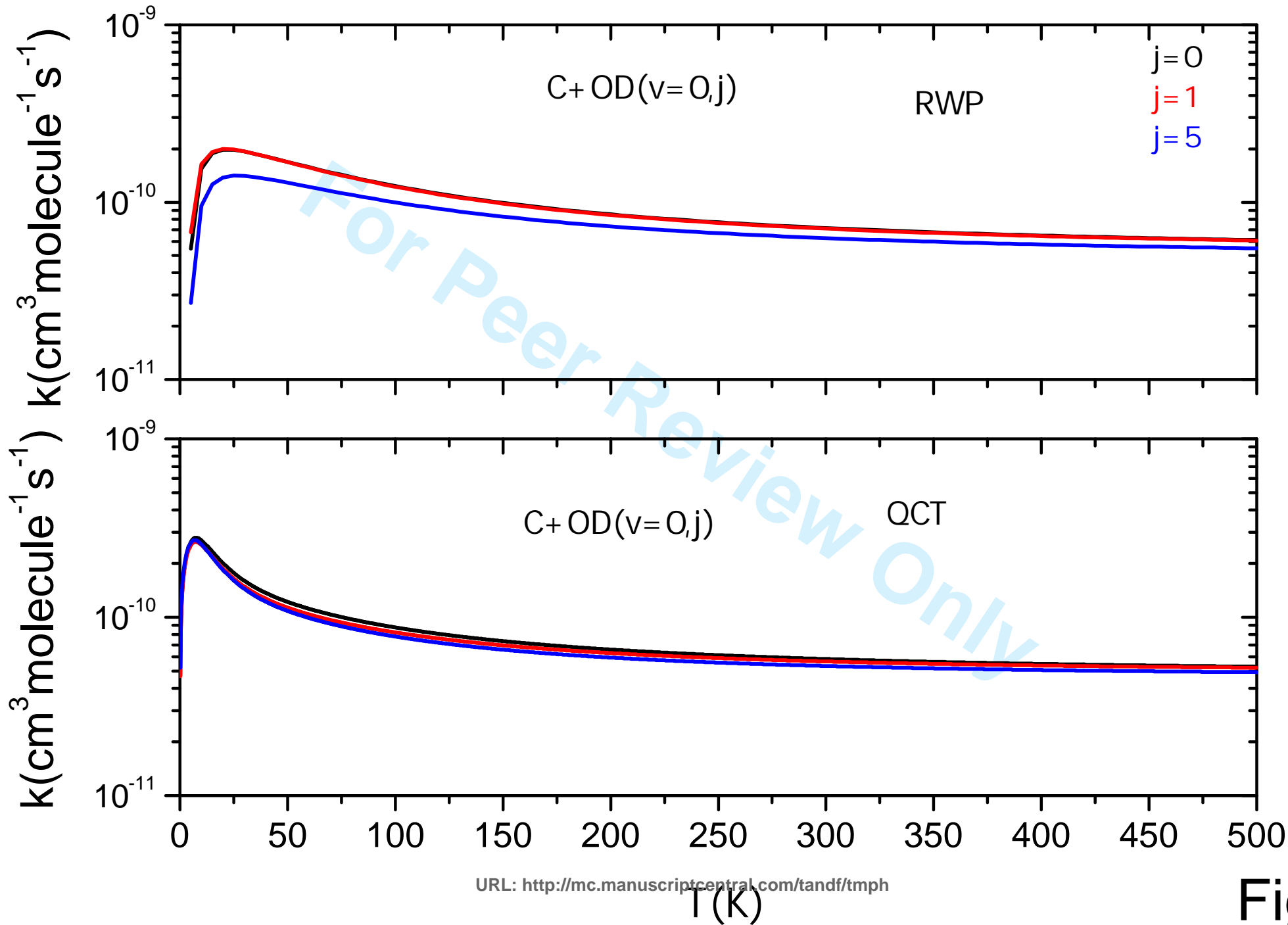


Fig.7

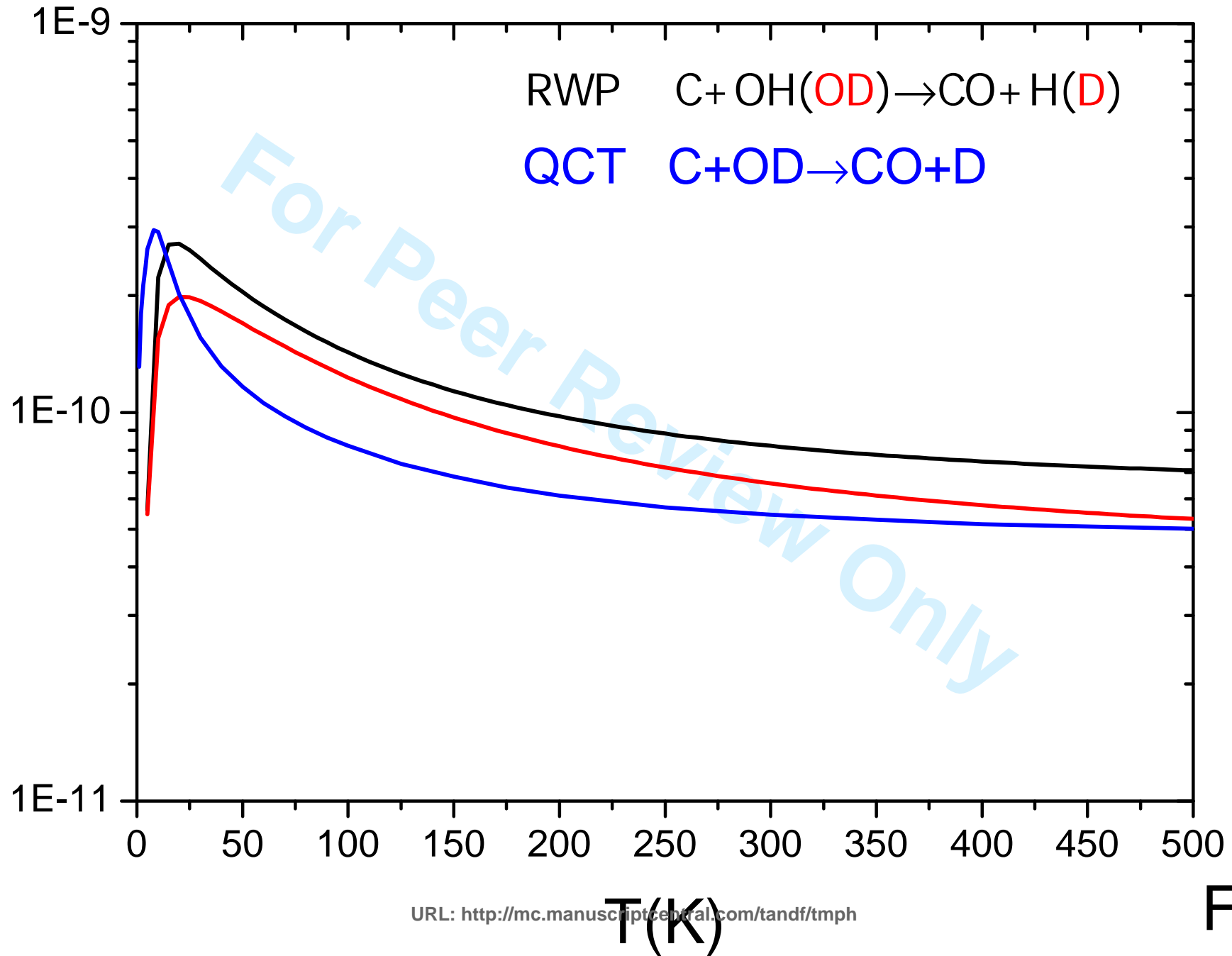


Fig.8

1  
2  
3 Pascal HONVAULT  
4 Institut UTINAM (UMR CNRS 6213)  
5 UFR Sciences et Techniques  
6 Université de Franche-Comté  
7 25030 Besançon cedex, France  
8 Tel: 33 (0) 3 81 66 64 84  
9 Fax: 33 (0) 3 81 66 64 75  
10 e-mail: pascal.honvault@univ-fcomte.fr  
11  
12

13  
14 Besançon, October 19 2010

15  
16 Professor Hans-Joachim Werner  
17 Editor, Molecular Physics  
18  
19  
20  
21  
22

23 Dear Professor Hans-Joachim Werner,  
24  
25  
26

27 We submit a new revised version of the manuscript "Influence of ro-vibrational and isotope  
28 effects on the dynamics of the  $C(^3P)+OD(X^2\Pi) \rightarrow CO(X^1\Sigma^+)+D(^2S)$  reaction".  
29 We thank the referee for his/her comments and remarks that have helped us to improve the  
30 presentation of the paper and helped the reader to a better understanding.  
31

32  
33 Sincerely yours,

34  
35 Pascal Honvault  
36  
37 -----  
38  
39

40 The C + OH reaction (and its isotopic variants) is known to take place (leading to formation  
41 of CO which is a key species) in interstellar medium, especially in cold and dense interstellar  
42 clouds (temperature around 10 K). This reaction is included in the international data bases  
43 such as UMIST, OSU, KIDA,... However crude (and often wrong) estimates of its rate  
44 constants are used in these data bases [see for instance Introduction in J. Chem. Phys. 126,  
45 184308 (2007)]. Furthermore, no experimental data are available on this system (very difficult  
46 system for experiments). So the rate constant at low temperature has to be computed using  
47 theoretical methods, such as quantum mechanical or quasi-classical trajectory methods.  
48  
49

50  
51  
52 The global fit of the potential energy surface is given in bond coordinates, and no problem  
53 was found.  
54

55 The reaction probability is less than 1 because inelastic processes take place too, as found in  
56 other OH + atom systems.  
57  
58

59 The method used in Ref. 4 is a statistical quantum wave packet method, that is more accurate  
60 than the standard Clary-Henshaw capture model, but in general less accurate than the quasi-

1  
2  
3 classical trajectory. Recently, we have published an article with a comparison of rate  
4 constants calculated using different capture methods [J. Phys. Chem. A 114, 7494 (2010)].  
5  
6

7 There is a discrepancy between the QCT and WP rotational distributions, already found in  
8 C+OH. The WP integral cross sections were obtained using a J-shifting method. Such an  
9 approximation may be appropriate for total or even vibrationally state-resolved cross sections,  
10 but the application of such a method to product rotationally state-resolved cross sections must  
11 be used with caution.  
12

13  
14 Page 4, section “II. Theory”, subsection “A. Real wave packet method”, after the last line  
15 (RWP integral cross sections and rate coefficients have been evaluated using the same  
16 methodologies as in Ref. [25].), we have added the following sentence: “WP calculations  
17 have been performed for total angular momentum  $J=0$ . A variant of the standard J-shifting  
18 method has been applied to estimate reaction probabilities for  $J>0$  and integral cross sections  
19 as a function of collision energy and rate coefficients have been calculated from the state-to-  
20 state reaction probabilities”.  
21  
22

23 We recall that the main goal of the paper is to present a comparison between WP and QCT  
24 results in order to exhibit some quantum effects, and a comparison between C+OH and C+OD.  
25 However, we agree with the referee and a complete analysis of the trajectories for both the  
26 C+OH/OD reactions will be done in a future study at several collision energies and for  
27 different rovibrational states of OH/OD. This QCT study (ICS, DCS, complex lifetime, ...)  
28 may help to understand (better than with capture models) the mechanisms involved in these  
29 reactions and the origin of differences found between the two isotopic systems.  
30  
31

32  
33 We have also considered the “minor comments” enumerated by the referee and corrected the  
34 text accordingly. One exception: we agree with the referee about the definition of the  
35 “excitation function”, but we keep the “excitation function” expression which is usually  
36 employed in the community.  
37

38 Fig. 4 and Fig. 5 have been modified.  
39  
40  
41  
42  
43  
44  
45  
46  
47  
48  
49  
50  
51  
52  
53  
54  
55  
56  
57  
58  
59  
60